Double Photoionization of Helium Down to 100 meV above Threshold

A. Huetz and J. Mazeau

Laboratoire de Spectroscopie Atomique et Ionique (UMR 8624 du CNRS), Université Paris-Sud, Batiment 350, 91405 Orsay Cedex, France

(Received 25 February 2000)

Double photoionization of helium has been studied using a new instrument which allows one to detect the two emitted electrons over 4π steradians and measure their individual momenta. The experiments have been performed at 0.2 and 0.1 eV above threshold, and both double and triple differential cross sections have been extracted. In comparison with higher energy data, the results show that the strength of angular correlation between the two electrons increases towards threshold.

PACS numbers: 32.80.Fb

The double escape of two electrons from an ionic core is a full three body process, which requires an intimate correlation between these electrons to avoid recapture of one of them. This is especially true close to threshold, where the kinetic energy is not able to balance the effects of the three body Coulomb interaction. Nearly half a century after the classical analysis of Wannier [1] *ab initio* quantum treatments of this fundamental process have appeared, such as the recent convergent close coupling (CCC) [2] and hyperspherical $\mathcal{R}$ matrix with semiclassical outgoing-wave (H$\mathcal{R}$M-SOW) [3] theories. Experimental data are therefore needed to test them, especially in the critical threshold region. In addition, recent experimental [4] and theoretical [5] studies of the helium spectrum within less than 1 eV *below* the double ionization threshold at 79 eV bring the question of continuity across the double ionization limit and call for investigations at less than 1 eV *above* threshold. But this region is a challenge for experimentalists as the yield of electrons is vanishingly small towards threshold.

Substantial progress has been made in this direction since the pioneering work of Schwarzkopf *et al.* [6]. Electron spectrometers [7–9] and conventional time of flight techniques [10] have been used to measure the so-called triple differential cross section (TDCS) with respect to the angles and energies of the two electrons from a few tens of eV down to 0.6 eV above threshold. More recently the cold-target recoil-ion momentum spectroscopy (COLTRIMS) technique has also provided TDCSs measurements down to 1 eV above threshold [11]. However, all these methods suffer from fundamental limitations when approaching very low energies of the emitted electrons. Perturbing fields are difficult to avoid in the field-free region where electrons propagate before entering electrostatic analyzers or drift tubes, and the relative energy resolution $\Delta E/E$ of the former deteriorates rapidly towards threshold. In the COLTRIMS method, the ion momentum spreading due to thermal motion is transferred to the electron momentum measurement resulting in a low energy limit for one of the two electrons (E_1 or E_2) and, therefore, the total excess energy above threshold ($E = E_1 + E_2$).

Here we report on a new method which avoids these technical restrictions and allows one to measure the six components of the two electron momenta $\mathbf{k}_1$ and $\mathbf{k}_2$. Briefly, the experiment, shown in Fig. 1, is based on position sensitive detectors (PSD) using microchannel plates and 2D multianodes [12]. Significantly, the detection system is able to locate particles separated by only 1.5 ns, which is an order of magnitude less than the dead time of delay line detectors. This experiment [*coïncidences entre ions et électrons localisés* (CIEL)], which has been previously used in the "ion mode" for molecular studies [13], is used here in the "electron mode" for the first time. The gas beam is crossed with the photon beam and a weak electric field of typically 2 V cm^{-1} is applied to the inner region by means of two plates drilled with holes of 10 mm diameter. Electrons passing the hole are further accelerated, and enter into a drift tube before being

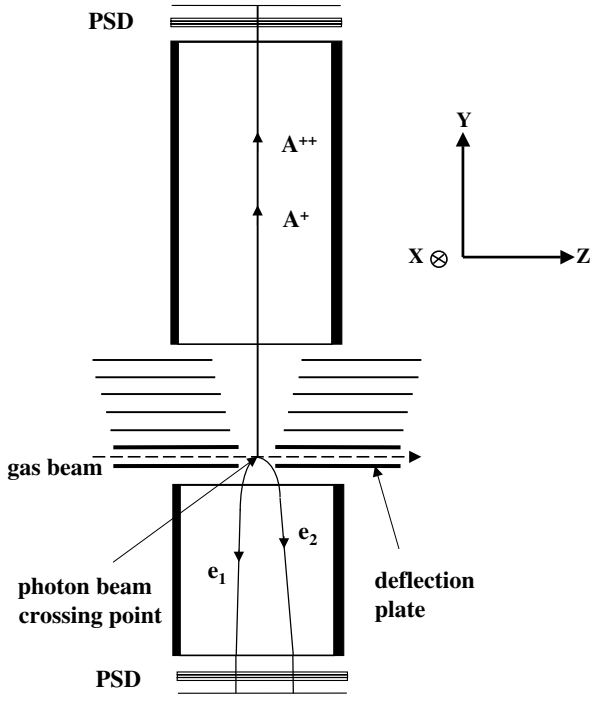

FIG. 1. Schematic diagram of the experimental setup.

 0031-9007/00/85(3)/530(4)$15.00

detected. Ions are similarly detected in the opposite tube and detector. The synchrotron source Super-ACO (France) has been used in the two bunches mode, allowing measurement of times of flight for all the particles. With reference to Fig. 1, the SU6 undulator line produces linearly polarized light propagating along the $\hat{\mathbf{X}}$ axis, with Stokes parameters $S_1 = 0.95, S_2 = 0, S_3 = 0$, and with the main axis of polarization, $\hat{\mathbf{Z}}$, in the horizontal plane. The $\hat{\mathbf{Y}}$ axis of the whole detection system is vertical for the present measurements, as this position can be shown to minimize the effects of detector dead time when measuring two electrons, thanks to the cylindrical symmetry around the horizontal $\hat{\mathbf{Z}}$ axis. The trajectories of electrons are simulated numerically, allowing one to extract the three momentum components k_x, k_y, k_z for each detected electron from the three measured quantities x, z, t. With an extraction field of 2 V cm^{-1}, electrons are collected over 4π steradians up to a kinetic energy of 150 meV. The energy and angular resolutions depend on time and position resolutions, and also on the modulus of $\mathbf{k}_1$ or $\mathbf{k}_2$ and its angle with the $\hat{\mathbf{Y}}$ detection axis. Typically for a 50 meV electron they remain below 10 meV and 8°. The ions are analyzed by their time of flight, but the position analysis, although possible, is not used in the present "electron mode." Times of flight are typically 80 ± 10 ns for the electrons, 5 μs for He^{++} ions, and are measured with respect to the photon pulses. The data are stored in the event mode, and for each detected double ionization event seven quantities (x, z positions of the two electrons and the times of flight of both electrons and the ion) are recorded. From these the six components of $\mathbf{k}_1$ and $\mathbf{k}_2$ are obtained, and further transformed to give the E_1 and E_2 energies of the two electrons, as well as their θ_1, θ_2 polar and ϕ_1, ϕ_2 azimuthal angles with respect to the $\hat{\mathbf{Z}}$ axis.

Two distinct experiments have been performed at photon energies of 79.2 and 79.1 eV, each having a photon resolution of 100 meV, and about 30 000 and 15 000 double ionization events were, respectively, recorded over about one week of beamtime each. As first established by Huetz *et al.* [14] the TDCS for linear polarization along $\hat{\mathbf{Z}}$ is given exactly by

$$\sigma_z^3 = |a_g(E_1, E_2, \theta_{12})\,(\cos\theta_1 + \cos\theta_2) + a_u(E_1, E_2, \theta_{12})\,(\cos\theta_1 - \cos\theta_2)|^2, \quad (1)$$

where θ_{12} is the angle between the two electrons. It has been subsequently observed [7,8,11] that when approaching threshold (i) the second amplitude vanishes, in agreement with Wannier [1], and (ii) that the first one becomes insensitive to E_1 and E_2 and depends only on the total excess energy above threshold E. Therefore we are left with

$$\sigma_z^3 = C_E(\theta_{12})\,(\cos\theta_1 + \cos\theta_2)^2. \quad (2)$$

Taking into account polarization of the light in the actual experiment [6] leads to $\sigma^3 = 0.975\sigma_z^3 + 0.025\sigma_y^3$ where σ_y^3 is given by an expression similar to Eq. (2) but with angles referred to the $\hat{\mathbf{Y}}$ axis. However, the second term does not influence appreciably the following analysis, and therefore we approximate σ^3 by σ_z^3. Integration over the whole space of Eq. (2) at constant θ_{12} gives $\cos(\theta_{12}/2)^2\, C_E(\theta_{12})$, the probability distribution of the mutual angle θ_{12}. The latter compares well with histograms of θ_{12} values extracted from the whole ensemble of events, excluding those with E_1 or $E_2 < 20$ meV, for which the angular resolution degrades too much. Fits of these histograms using the Gaussian shape of the correlation factor [14]

$$C_E(\theta_{12}) = a(E)\exp\left(-\frac{4\ln 2(\theta_{12} - 180)^2}{\gamma^2}\right) \quad (3)$$

give $\gamma = 57 \pm 4°$ and $\gamma = 60 \pm 4°$ at $E = 100$ and 200 meV, respectively, where γ is the FWHM of the Gaussian. Similarly, the asymmetry parameter β which characterizes the angular distribution of electrons can be obtained from histograms of θ_1 or θ_2 angles, leading to $\beta = -0.65 \pm 0.1$ at $E = 100$ meV and $\beta = -0.60 \pm 0.1$ at $E = 200$ meV. Going one step further, TDCSs for coplanar geometry can be derived by selecting events where the vectors $\mathbf{k}_1$ and $\mathbf{k}_2$ are coplanar with the $\hat{\mathbf{Z}}$ axis, within $\phi_1 - \phi_2 = \pm 20°$. The cylindrical symmetry of the electron pair around the $\hat{\mathbf{Z}}$ axis allows integration over azimuthal angle, and we obtain the absolute TDCSs from a procedure similar to that already detailed in COLTRIMS experiments at higher energy [15]. In the present case we use integral cross sections derived from the law $\sigma^{++} = 1.02E^{1.05}$ kb [16].

The results for the lowest energy $E = 100$ meV are reported in Fig. 2, where three different angles $\theta_1 = 90°$, 60°, and 30°, have been selected. From Eq. (2) the angular patterns for $\theta_1 = 120°$ and 150° are expected to be mirror images of those at 60° and 30°, respectively. This is very well verified by the experiment, and is an important consistency check of the whole experimental procedure. We have used this property in Fig. 2, by averaging $60^{\circ}/120^{\circ}$ (b) and 30°/150° (c) data to improve the statistics. At $\theta_1 = 0°$ the number of events becomes too small to be significant, due to the solid angle effect already stressed in [15] and also to the low values of γ, which make the TDCS decrease very rapidly with θ_1.

The acceptance bandwidths are ±10° for θ_1, ±2.5° for θ_2, and the selected energies are $E_1 = 50 \pm 30$ meV and $E_2 > 20$ meV. The full curves in Fig. 2 are based on Eqs. (2) and (3) after normalization to the $\theta_1 = 90°$ pattern, and with $\gamma = 57°$ as deduced from all events. Excellent agreement is evident in Figs. 2(a) and 2(b) regarding the shapes and intensities of the two lobes patterns. In Fig. 2(c) the statistics become poorer, and a slight discrepancy is observed. However, a good agreement is restored by using $\gamma = 54°$ as shown by the dotted curve, which is still consistent with the 57° ± 4° result based on the whole set of 15 000 events. The scaling coefficient $a(E)$ used in Fig. 2 is 590 b eV^{-1} sr^{-2}, but it is underestimated

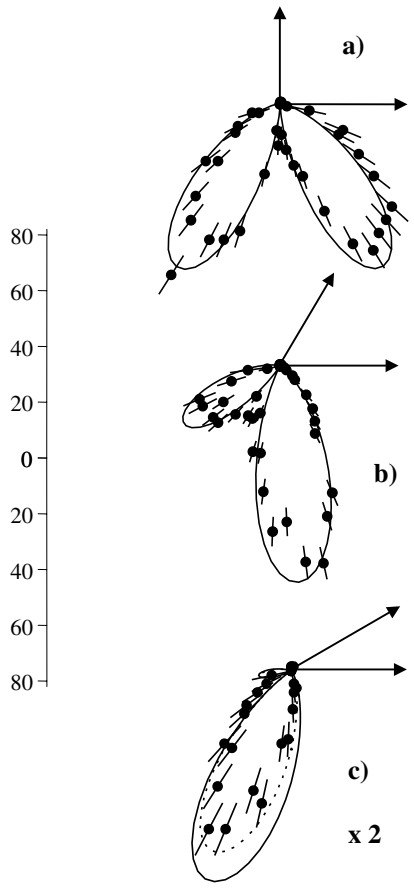

FIG. 2. Coplanar TDCSs at $E = 100$ meV. The arrow to the right indicates the main axis of linear polarization $\hat{\mathbf{Z}}$. The other arrow gives the direction of the first electron. The angle between them is $\theta_1 = 90°$ (a), 60° (b), and 30° (c). The absolute scale in polar coordinates is given in barns $\mathrm{eV}^{-1}\,\mathrm{sr}^{-2}$, and is common to all three cases. The (c) distributions (both experiment and calculations) have been multiplied by 2.

as the experimental resolutions and bandwidths have not been included [a more precise evaluation of $a(E)$ will be presented elsewhere].

Although not shown here, similar conclusions can be drawn from our results at 200 meV above threshold, which show an even better agreement between Eqs. (2) and (3) with $\gamma = 60°$ and coplanar TDCSs. Therefore the present findings appear to be internally consistent and give for the first time a precise measure of the strength of angular correlation down to 100 meV above threshold.

Comparing our results with previous experimental and theoretical studies, Fig. 3 summarizes the values of γ (a) and β (b) parameters previously reported in the 0–20 eV energy range, using a logarithmic energy scale. Because of our 100 meV photon bandwidth and the strongly varying cross section at threshold, the centroid of $E_1 + E_2$ distributions is observed to be slightly shifted up with respect to photon energy, and accordingly our results are plotted at 116 and 209 meV. It was already known that γ decreases smoothly from about 91° at 20 eV down to about

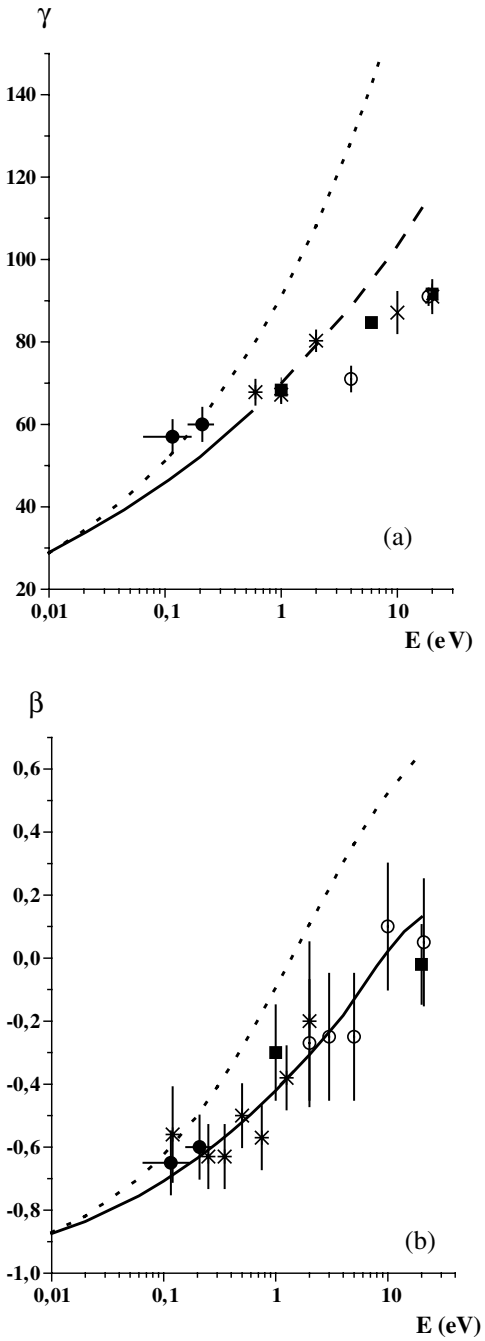

FIG. 3. Evolution of γ (a) and β (b) parameters with photon energy. The dotted curves are derived from the semiclassical Wannier theory [22], and the full curve shows the H$\mathcal{R}$M-SOW theory [3]. The reported experimental results are (a) full circles: present work (the horizontal bars account for our 100 meV photon energy bandwidth); squares: from [11]; open circles: from [17]; stars: from [8]; crosses: from [6]; triangle: from [9]. Note that at 20 eV, Refs. [6,9] give the same value 91°, and that Ref. [17] gives 91° at 18.6 eV and Ref. [11] 91.6° at 20 eV. (b) full circles: present work; squares: from [18]; open circles: from [19]; stars: from [20].

68° at 1 eV (67° ± 2° [8] and 68.3° ± 3° [11]). Our value of 57° ± 4° at 0.1 eV demonstrates that this evolution goes on at lower energies, although it appears to be rather

slow. Such evolution of angular correlation below 1 eV was questioned on the basis of β parameter measurements [stars in Fig. 3(b) from [20]]. Our own β values reported in Fig. 3(b) are consistent with the latter, but our more accurate γ measurements, which for the first time reach energies as low as 0.2 and 0.1 eV, definitely show that the strength of angular correlation keeps increasing towards threshold. Note that the present β data include various energy sharings, in contrast with [20] where asymmetric conditions were selected. The question of a β dependence to energy sharing was raised in [21], but there is no evidence of such an effect in Fig. 3(b).

The dotted curves in Fig. 3 display the $\gamma = 91\,E^{0.25}$ law and associated β from semiclassical analysis [22] based on Wannier's classical threshold theory [1]. It was stressed when the first TDCSs measurements were reported [6] that this law overestimates γ by nearly a factor of 2 at 20 eV. This is not so surprising, as the Wannier threshold law is known to apply only up to about 2 eV [16]. However, another discrepancy appears clearly in Fig. 3(a), which is more significant as it occurs in the 0.1–1 eV energy range. The $0.91\,E^{0.25}$ law gives $\gamma = 60.8°$ at 0.2 eV, in good agreement with our $60 \pm 4°$ value, but clearly overestimates the 1 eV data and decreases too rapidly in this energy range. The recent H$\mathcal{R}$M-SOW calculations [3], giving predictions down to 0.01 eV, are shown in Fig. 3. Although in good agreement with experiments at a few eV down to 1 eV, they underestimate γ values at low energy and seem to decrease again too rapidly towards zero. Such effects cannot be distinguished on the less accurate β measurements, where H$\mathcal{R}$M-SOW are entirely consistent with experiments over the whole energy range. It is finally worth remarking that in Fig. 3(b) the asymptotic $\beta = -1$ limit is still far from being reached at 100 meV, and is approached within 10% only at 10 meV, according to theoretical predictions.

To summarize, the new experimental technique presented here allows measurements of TDCSs at threshold, over the whole momentum space. It has been applied to helium at energies which are a challenge for theoretical studies, which we hope will be stimulated. On the experimental side the present method will be used to study other atomic and molecular systems. It will also be extended to lower energies, as there is no obstacle to decrease the electric field down to a few hundred $\mathrm{mV\,cm^{-1}}$ and to analyze electrons in the energy range of a few meV.

Michel Lavollée has played a leading role in the development of CIEL experiment and PSD detectors, which made the present work possible. It is a pleasure for us to thank him warmly for his essential contribution. We are also very grateful to Tim Reddish, Laurence Malegat, and Patricia Selles for their precious help with the manuscript.

[1] G. H. Wannier, Phys. Rev. **90**, 817 (1953).
[2] A. S. Kheifets and I. Bray, J. Phys. B **31**, L447 (1998).
[3] L. Malegat, P. Selles, and A. Kazansky, Phys. Rev. A **60**, 3667 (1999).
[4] M. Domke, K. Schulz, G. Remmers, G. Kaindl, and D. Wintgen, Phys. Rev. A **53**, 1424 (1996).
[5] B. Grémaud and D. Delande, Euro. Phys. Lett. **40**, 363 (1997).
[6] O. Schwarzkopf, B. Krässig, J. Elmiger, and V. Schmidt, Phys. Rev. Lett. **70**, 3008 (1993); O. Schwarzkopf and V. Schmidt, J. Phys. B **28**, 2847 (1995); J. Phys. B **29**, 1877 (1996).
[7] P. Lablanquie, J. Mazeau, L. Andric, P. Selles, and A. Huetz, Phys. Rev. Lett. **74**, 2192 (1995).
[8] G. Dawber, L. Avaldi, A. G. McConkey, H. Rojas, M. A. MacDonald, and G. C. King, J. Phys. B **28**, L271 (1995).
[9] J. P. Wightman, S. Cvejanovic, and T. J. Reddish, J. Phys. B **31**, 1753 (1998).
[10] J. Viefhaus, L. Avaldi, F. Heiser, R. Hentges, O. Gessner, A. Rüdel, M. Wiedenhöft, K. Wieliczek, and U. Becker, J. Phys. B **29**, L729 (1996).
[11] R. Dörner, H. Bräuning, J. M. Feagin, V. Mergel, O. Jagutzki, L. Spielberger, T. Vogt, H. Khemliche, M. H. Prior, J. Ullrich, C. L. Cocke, and H. Schmidt-Böcking, Phys. Rev. A **57**, 1074 (1998).
[12] M. Lavollée, Rev. Sci. Instrum. **70**, 2968 (1999).
[13] M. Lavollée and V. Brems, J. Chem. Phys. **110**, 918 (1999).
[14] A. Huetz, P. Selles, D. Waymel, and J. Mazeau, J. Phys. B **24**, 1917 (1991).
[15] H. Bräuning, R. Dörner, C. L. Cocke, M. H. Prior, B. Krässig, A. S. Keihfets, I. Bray, A. Bräuning-Demian, K. Carnes, S. Dreuil, V. Mergel, P. Richard, J. Ullrich, and H. Schmidt Böcking, J. Phys. B **31**, 5149 (1998).
[16] H. Kossmann, V. Schmidt, and T. Andersen, Phys. Rev. Lett. **60**, 1266 (1988).
[17] L. Malegat, P. Selles, P. Lablanquie, J. Mazeau, and A. Huetz, J. Phys. B **30**, 263 (1997).
[18] H. Bräuning, R. Dörner, C. L. Cocke, M. H. Prior, B. Krässig, A. Bräuning-Demian, K. Carnes, S. Dreuil, V. Mergel, P. Richard, J. Ullrich, and H. Schmidt-Böcking, J. Phys. B **30**, L649 (1997).
[19] R. Wehlitz, F. Heiser, O. Hemmers, B. Langer, A. Menzel, and U. Becker, Phys. Rev. Lett. **67**, 3764 (1991).
[20] G. Dawber, R. I. Hall, A. G. McConkey, M. A. MacDonald, and G. C. King, J. Phys. B **27**, L341 (1994), and references therein on previous measurements.
[21] F. Maulbetsch and J. S. Briggs, Phys. Rev. Lett. **68**, 2004 (1992); J. Phys. B **26**, 1679 (1993).
[22] J. M. Feagin, J. Phys. B **17**, 2433 (1984).